Article:
Stott, D, Boyd, DS, Beck, A et al. (2015) Airborne LiDAR for the detection of archaeological vegetation marks using biomass as a proxy. Remote Sensing, 7 (2). 1594 - 1618. ISSN: 2072-4292

https://doi.org/10.3390/rs70201594

Remote Sens. **2015**, *7*, 1594-1618; doi:10.3390/rs70201594

OPEN ACCESS

remote sensing

ISSN 2072-4292

www.mdpi.com/journal/remotesensing

Article

Airborne LiDAR for the Detection of Archaeological Vegetation Marks Using Biomass as a Proxy

David Stott [1], Doreen S. Boyd [2,*,†], Anthony Beck [1,†] and Anthony G. Cohn [1]

[1] School of Computing, University of Leeds, Leeds LS9 2JT, UK; E-Mails: scds@leeds.ac.uk (D.S.); a.r.beck@leeds.ac.uk (A.B.); a.g.cohn@leeds.ac.uk (A.G.C.)

[2] School of Geography, University of Nottingham, Nottingham NG7 2RD, UK

† These authors contributed equally to this work.

* Author to whom correspondence should be addressed; E-Mail: doreen.boyd@nottingham.ac.uk; Tel.: +44-115-951-4182; Fax: +44-115-951-5249.

Academic Editors: Rosa Lasaponara and Prasad S. Thenkabail

Received: 16 July 2014 / Accepted: 26 January 2015 / Published: 3 February 2015

Abstract: In arable landscapes, the airborne detection of archaeological features is often reliant on using the properties of the vegetation cover as a proxy for sub-surface features in the soil. Under the right conditions, the formation of vegetation marks allows archaeologists to identify and interpret archaeological features. Using airborne Laser Scanning, based on the principles of Light Detection and Ranging (LiDAR) to detect these marks is challenging, particularly given the difficulties of resolving subtle changes in a low and homogeneous crop with these sensors. In this paper, an experimental approach is adopted to explore how these marks could be detected as variations in canopy biomass using both range and full waveform LiDAR data. Although some detection was achieved using metrics of the full waveform data, it is the novel multi-temporal method of using discrete return data to detect and characterise archaeological vegetation marks that is offered for further consideration. This method was demonstrated to be applicable over a range of capture conditions, including soils deemed as difficult (*i.e.*, clays and other heavy soils), and should increase the certainty of detection when employed in the increasingly multi-sensor approaches to heritage prospection and management.

Keywords: archaeology; Airborne LiDAR/Laser Scanning; vegetation marks; arable

1. Introduction

Near-surface archaeological residues that present themselves as features in the vegetated landscape are usually the result of anthropogenic interference with the natural soil matrix [1]. This interference causes differences in the composition and structure of the soil and these, in turn, influence the development and health of any vegetation present on the surface. Such changes can be manifested in vegetation canopy properties (generically known as crop marks) and used as a proxy for changes in the soil caused by past human activity [2,3]. However, the formation of archaeological vegetation marks is a complex process that is related to many factors, such as the physical (including thermal), chemical and biological properties of the soil; environmental dynamics during the crop lifecycle; soil-moisture balance; growth characteristics and requirements of the vegetation and land-management processes [4]. Moreover, these processes operate at different scales and interact in complex ways to influence the development and health of overlying vegetation, presenting in terms of structure and density (such as Leaf Area Index (LAI) and canopy biomass), or as variations in stress and vigour expressed as changes in pigmentation (such as variations in senescence) under the right conditions [5–7].

These principles are widely used to detect archaeological landscapes using visible wavelength photography from airborne platforms [8]. However, this is over-reliant on the visual component of the electromagnetic spectrum [9,10]. Furthermore, there are types of soil (e.g., clay or other heavy soils), crops, and environmental conditions that make it difficult to detect archaeological features proxied as crop marks in this way. In areas where this difficulty is persistent, this means a bias in detection, which becomes a bias in coverage. This fragments the knowledge base, leading to less than optimal management and policy decisions [11,12]. Therefore, an alternative approach to archeological prospection via vegetation marks in such "difficult" areas is imperative [13]. Other remote sensing devices and modes of operation have the potential to improve detection of archaeological residues, as their ability to detect subtly expressed contrasts could afford the opportunity to both extend the temporal window for detection and detect subtly expressed features that cannot be detected using conventional photography [3]. There has been some success in using alternative sensors [14,15] and much recent attention has been placed on the use of airborne LiDAR (also known as Airborne Laser Scanning, based on the principles of Light Detection and Ranging).

Airborne LiDAR is now widely used in archaeology [16,17]) and, in particular, to detect features defined by slight changes in land surface topography, as these sensors enable these topographic changes to be detected regardless of the vegetation cover on that surface via the production of digital terrain models (DTM) [18–21]. Airborne LiDAR has not been employed for vegetation mark identification via a digital surface model (DSM). This is probably because, although in theory a single airborne LiDAR survey can provide both the DSM and the DTM by using the first and last returns respectively, often the vegetation is either of limited height or exhibits a limited dynamic range (the difference between the maximum and minimum values) [22]. Thus, the production of a vegetation canopy height model to identify changes in its properties related to changes in the soil as a result of archeological residue is extremely challenging. Consequently, archeological prospection via the vegetation canopy has primarily focused on using intensity, rather than the range measurements of airborne LiDAR.

A LiDAR instrument is an active sensor emitting a pulse, generally at a single narrow wavelength in the near-infrared. The backscattered pulse contains an intensity component that can be crudely

considered as a single narrow bandwidth imaging spectrometer. As such, Challis *et al.* [23,24] used the intensity values to detect both archaeological and geological crop marks and Briese *et al.* [25,26] demonstrated a significant improvement in detection using the intensity data centered at 550 nm from an airborne LiDAR instrument array employing multiple wavelengths. Briese *et al.* also employed the full waveform (FWF) recorded by an airborne LiDAR with some success. It is well established that, via advanced processing methods (e.g., signal decomposition or modelling [27]), FWF data offers increased pulse detection reliability, accuracy, and resolution and, therefore, improves the accuracy of topographic models that could be used for archaeological detection [28–30]. Furthermore, these data have been shown to provide additional information about the structure and physical backscattering properties of the objects they interact with [31]. In particular, significant information on the roughness, slope and reflectivity of surface materials may be retrieved from full waveform data (using both the range and intensity data). For example, differences in the properties of isolated echoes (e.g., width, amplitude or cross-section) and their number (e.g., echo ratio) have been found for vegetation and ploughed fields *versus* roads, or meadow areas and between grass and bare earth, or between different roof materials [32,33]. Common application of these data have been in forest studies, both at the level of the stand and the individual tree, for the estimation and modelling of forest properties [34] and tree species mapping [35]. It is commonly assumed that for studies other than that of forests, FWF LiDAR cannot be expected to enhance the information content already provided by the discrete return data [36]. However, Doneus *et al.* [28] have used FWF for the detection of archaeological features in a forest understory and produced improved detection confidence over discrete returns.

In this paper, it is hypothesised that, via a fuller use of airborne LiDAR data, archaeological features could be detected using the vegetation canopy itself as a proxy (*i.e.*, as vegetation marks) for archaeology. Two approaches are investigated: (i) the production of a canopy height model (CHM) produced via multiple-date discrete LiDAR data and (ii) the use of canopy biomass metrics extracted from the full waveform of a single-date dataset. A CHM is quite simply a DSM minus the corresponding DTM (or bare earth model); in this paper, we suggest that taking the DSM and DTM from different airborne LiDAR surveys (*i.e.*, exploiting the multi-temporal domains of remote sensing) overcomes the issues associated with dynamic range, and we demonstrate that the CHM can show contrast relating to soil changes caused by archeological remains. In addition, we suggest that the extra information provided by the full waveform may also exhibit patterns relating to changes in vegetation canopy properties that are caused by the occurrence of archaeological residues in the soil. The two approaches under investigation in this paper have the potential to extend the utility of airborne LiDAR surveys for archaeological prospection in general. But, in particular, our overriding objective is to determine how airborne LiDAR might improve archaeological prospection in "difficult" conditions (*i.e.*, clay soil); improved detection over "difficult" areas is a research priority and, if successful, should afford improved detection of archaeological features in the UK and beyond.

2. Study Area and Data

2.1. Background to Study

This work forms part of the Detection of Archaeological Residues using remote sensing Techniques (DART) project. DART was initiated in 2010 in order to investigate the ability of various sensors to detect archaeological features in "difficult" circumstances [37]. DART has the overall aim of developing analytical methods for identifying and quantifying gradual changes and dynamics in sensor responses associated with surface and near-surface archaeological features under different environmental and land-management conditions. "Identification" and "quantification" concerns the differentiation of archaeological sediments from non-archaeological strata on the basis of remotely detected phenomena (e.g., resistivity, dielectric permittivity, crop growth, thermal properties *etc.*). An experimental approach has been taken whereby monitoring equipment (to measure precipitation, soil and air temperature, and soil apparent dielectric permittivity and bulk electrical conductivity) has been installed in known archaeological features at two locations in southern England. Regular remote sensing surveys were taken over these test sites, including multi-temporal airborne imaging spectroscopy, airborne LiDAR and aerial photography by the UK's NERC Airborne and Remote Survey Facility.

2.2. Study Area

The two UK locations at which DART are focused are Diddington in Cambridgeshire and Harnhill in Gloucestershire (see Figure 1). Harnhill experiences significantly more rainfall than Diddington, though it should be noted that 2011 had a particularly dry spring and the summer of 2012 was significantly wet [38]. Both locations contain known archaeology within the two investigation areas, identified from local historic environment records and map regression. Both areas are agricultural but have different planting and rotation practices. At each site, two areas of interest (named fields) were chosen, one on clay (*i.e.*, a "difficult" location where discrimination of archaeological features might be poor due to heavy soils) and the other on free-draining geology (where archaeological features should be more easily differentiated from the background).

Diddington is on Oxford Clay with the "DDT1" field having free-draining river terrace deposits and the "Clay" field having mid-Pleistocene till. On both fields at Diddington, the archaeological features are enclosure ditches from an extensive late prehistoric and Romano-British settlement complex. At Harnhill, the "Cherry Copse" field is directly located on limestone cornbrash with the "Quarry" field on a clayey signet member (see Figure 1). At Quarry field, the archaeology comprises the remains of a Medieval and later open field system defined by ridge and furrow cultivation, bisected by a Post-Enclosure field boundary running SW-NE across the area. At Cherry Copse, the feature is a substantial post-medieval boundary ditch. None of the archaeological features at the four fields exhibit any topographic expression.

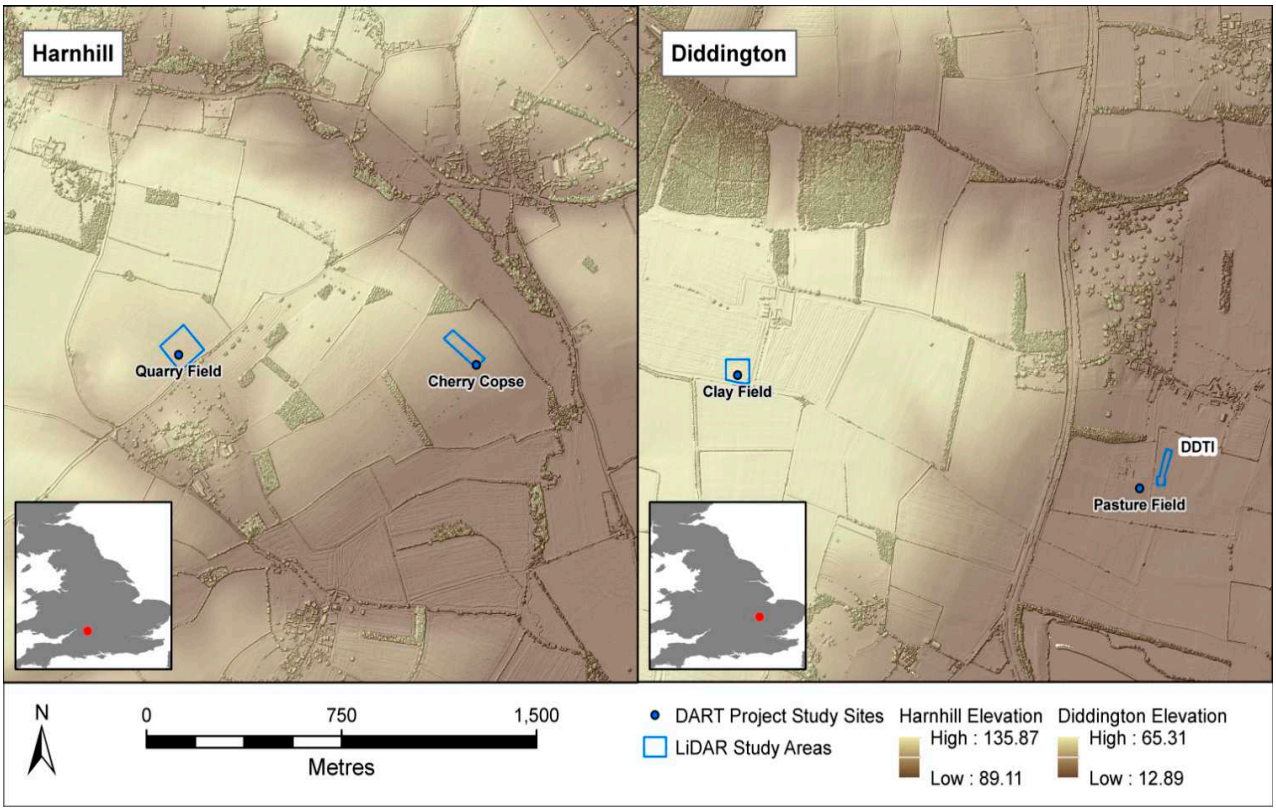

Figure 1. The two locations in southern England at which the study was undertaken, Harnhill and Diddington. At each location, two fields containing archaeological residues which do not exhibit any topographic expression were the focus of study using airborne LiDAR (illustrated by blue boxes).

2.3. Data Acquisition

Two sets of data were acquired: (i) airborne LiDAR data, which were the focus of the analyses and (ii) benchmark data used to explain any archeological residues revealed by the LiDAR analyses.

2.3.1. Airborne LiDAR Data

Airborne LiDAR data was acquired in every case using the same Leica ALS50-II small footprint system. At 1000 m, the footprint of the pulse is 22 cm, with a wavelength centered on 1064 nm. This sensor has capabilities for discrete and, from 2012, full waveform recording. Table 1 summarises the acquisition parameters for each set of LiDAR data captured. In every case, the direction of flight was in the east-west direction with each flightline being 260 m in width and the archaeological feature under investigation located from the centre to the bottom of the flight line in which it was captured. Geo-referencing was performed on the raw data by NERC ARSFDAN using the RTK, GNSS, and IMU sensors also on the platform. These data are available at http://dartportal.leeds.ac.uk/dataset/ [39].

Table 1. ALS surveys undertaken by the NERC ARSF Leica ALS50-II small footprint system at each site (*14 June 2011 survey is for Diddington only).

Flight Date	Provider	Sensor	Hits per m^2	Full-Waveform
14 June 2011 *	NERC ARSF	Leica ALS50	12	No
23 March 2012	NERC ARSF	Leica ALS50	12	Yes
20 June 2012	NERC ARSF	Leica ALS50	12	Yes

2.3.2. Benchmark Data

Three sets of benchmark data were collected in addition to the airborne LiDAR data. The first was comprised of a fluxgate gradiometer magnetometer survey, undertaken using either a Bartington Grad 601-2 or a Geoscan FM256 collected at a 0.25 m sample interval along 1 m traverses and located using RTK GNSS in each field. In addition to this geophysical survey to identify archaeological features, the study areas were captured using aerial photography (at a nominal resolution of 10 cm) with a Leica RCD105 survey camera simultaneously with each of the airborne LiDAR data acquisitions [39]. In addition to these aerial photographs, there was also a baseline aerial survey undertaken by the Geomatics Group Ltd. on the 27th of June 2011 and 8-bit RGB, 0.2 m spatial resolution data provided orthorectified to sub pixel accuracy [39]. The geophysical surveys were used for the statistical analysis of the vegetation marks, as using features identified solely as vegetation marks from aerial photography survey risks confirmation bias. The final set of benchmark data noted the vegetation type and growth state of the crop in the field at each site. For the 2012 airborne LiDAR acquisitions, temporally coincident 10–15 m long transects were established centered on (but running orthogonal to) a known archaeological feature in each of the four fields (where access allowed). The transects were sampled every 0.25 m for vegetation height and LAI, the latter using an Accupar LP-80 canopy ceptometer. This was conducted to provide physical measurement of the vegetation canopy in terms related to its biomass [40], to be used in conjunction with the known spatially coincident archaeology as explanation of any patterns in the airborne LiDAR data.

3. Methods

3.1. Data Processing

The airborne LiDAR data were supplied in the LAS format and converted to ASCII format using the LAStools software package. For the discrete data, captured on the three dates (Table 1), the entire point cloud was interpolated to a 0.4 m grid using the inverse distance weighted interpolation functions of the GDAL software library. Subsequently, the first discrete return data were used to produce a digital surface model (DSM) via the nearest neighbor value per grid cell for each date of acquisition and each study site. The spatial accuracy of the resultant geo-referenced DSMs was evaluated using the ortho-photography provided by the Geomatics Group Ltd and all had sub-pixel accuracy. The height values from the interpolated DSMs produced were compared over areas of hard standing at each site, and found to be consistent within 0.04 m. The full waveform data were interpolated using the same method. However, it was not possible to mitigate for the effects of scan-angle on the data, as the intensity values returned by the sensor are affected by the automatic gain control applied to the returning signal by the sensor. To reduce the impact of this, subsets of the FW data were derived from single flightlines, as near as possible

to the centre of the flightline. The full waveform ALS data captured over the fields at both Diddington and Harnhill in March and June 2012 were extracted and analysed using bespoke Python software [41]. All waveforms were smoothed using a univariate spline to remove noise. The locations of peaks in the waveform were identified using the change in the first derivative. These locations were used to segment the waveform. In all cases, only one peak was identified for each waveform. From this the three metrics of the (i) sum of intensity within the peak; (ii) maximum intensity of the peak, and (iii) overall width of the peak, were extracted.

Any magnetic anomalies present in the magnetometer survey data were interpreted as likely to be caused by archaeological and geological features and digitized as polygons. These polygons were then converted to rasters using the GDAL software library and used to classify each pixel in the raster models derived from the LiDAR data. The aerial photography captured by the NERC ARSF were used to create an ortho-photographic mosaic of the study area using the AgiSoft PhotoScan Structure from Motion (SFM) package, using the EXIF data collected with the images to estimate camera position and exterior orientation parameters. The resultant 16-bit RGB ortho-photographic mosaics are of 0.1 m spatial resolution, and georeferenced to +/− 0.2 m accuracy. The spatial resolution of the images is so high, it is difficult to identify variations on a canopy scale. In order to facilitate this, Gaussian smoothing filtering was applied to generalize the crop canopy and improve the acuity of the features. Both these aerial photographs and the Geomatics Group's ortho-photography were further processed; to compare with the LiDAR data, the Normalized Difference Green Red Index (NDGRI = (G − B)/(G + B), where G and R are the green and red bands respectively) was computed in order to maximise any contrast observed.

3.2. Data Analyses

Each site was surveyed on different dates with the vegetation in a different state each time. By processing this data appropriately, a DTM could be created that represented a "bare earth surface", and a DSM could be created that represented a "mature vegetation surface" which could afford the calculation of a canopy height model (CHM). Since the LiDAR data acquired during March 2012 occurred when there was bare soil or very immature vegetation this was used as the DTM for each of the four fields under investigation. This "bare earth" DTM model was pre-processed using a uniform low-pass filter with an 11 × 11 kernel size. This was chosen to smooth out variations in the cultivated surface by tillage, and the texture of the immature crop (particularly brassicas), which can produce spurious anomalies in the resultant model. The DEMs generated from the surveys undertaken when the crop was mature (*i.e.*, June 2011 and June 2012) were used as a DSM in the generation of the CHM. Each of these DSMs was pre-processed using a median filter with a 3 × 3 kernel size to remove noise and small scale variations in the crop canopy, *i.e.*, to look for major biomass/height differences as proxies for archaeological prospection.

In order to evaluate the results from the airborne LiDAR analyses, a benchmark needed to be established for "known" archaeology. This benchmarking data was drawn from ground geophysical, aerial, photographic, and ancillary data collected as part of the DART project. The geophysical surveys were used for the statistical analysis of the vegetation marks, as using features identified solely as vegetation marks from aerial photographic surveys risks confirmation bias. Both the resultant multi-temporal LiDAR-derived CHMs and the extracted LiDAR FWF metrics were quantitatively assessed for archaeological prospection using a Welch's T-Test. Principal focus was on those areas in

the four fields where there is known archaeology as confirmed by the magnetometer survey data. Here the returns over the known archaeology are compared with that over background, thus determining the significance of contrast. This was conducted using a 16 × 16 pixel (3.4 m radius) kernel/moving window for each pixel that corresponds to the known archaeological features as revealed by the magnetometer survey in each field. Visual comparisons between the LiDAR data and the aerial photography were then undertaken, since this allowed the comparison of archaeological feature omission and commission between the different sensors in different contexts. This comparison enables the determination of the potential impact of the approach in different contexts in terms of detection complementarity, and how the approach addresses biases or deficiencies in current detection techniques.

To test the suitability of this methodological approach, a test on an area of unknown archaeological potential, located approximately 200 m west of Harnhill Quarry Field using data acquired on the 20th of June 2012, was undertaken. The area was under a flowering crop of winter wheat during this period, and no vegetation marks were visible on the ground surface. No archaeological features had been identified in this area. Here, we used the multi-temporal LiDAR-derived CHM, and the NDGRI index derived from the RGB June 2011 ortho-imagery was used for comparison. Both datasets were examined under a variety of histogram stretches and those features interpreted as being of likely archaeological origin were digitized.

4. Results

The benchmark data collected on vegetation type and growth state of the crop (Table 2) demonstrates that the multi-temporal airborne LiDAR surveys occurred under different localised cropping conditions. During the March 2012 survey, the fields were close to being "bare earth" and in June 2011 and 2012, the fields had mature vegetation.

Figure 2 presents the results from the magnetometry and the aerial photography surveys, and Figure 3 profiles the variations in canopy height and Leaf Area Index (LAI) measurements along the transects of the June surveys. These provide evidence of where the archeological residues were at these sites and, in the case of the profiles, demonstrate that both the Quarry field (spring wheat over clay) and Cherry copse field (pasture) at Harnhill showed an increase in both the LAI and canopy height over the archaeological features. There was some evidence of a change in LAI over archaeology at Clay field in Diddington (winter wheat over clay), which was not the case for canopy height. This indicated that, in this instance, vegetation biomass (related to LAI and height) is a sensitive indicator of archaeological presence. These areas were then the focus of investigation using (i) the airborne LiDAR-derived Canopy Surface Model and (ii) the biomass sensitive metrics derived from full-waveform data.

4.1. Archaeological Detection via the Multi-Temporal Airborne LiDAR Derived Canopy Height Model

The resultant multi-temporal airborne LiDAR-derived CHMs are displayed in Figures 4–7. In these figures, the clearest contrast between the neighboring pixels is indicated when there is red in both the *T*-value and *P*-value images, and it is at these locations that archaeological residues are proxied. At Diddington T1 (Figure 4), the tall canopy seen in June 2012 for the oilseed rape crop (much of which exceeded 1 m in height) did not exhibit readily discernable crop marks; however, there were some occurrences where the CHM model showed contrast which was not apparent in the aerial photographs,

in particular the round features in the south west corner. Conversely, the June 2011 winter wheat crop gave rise to much more contrast over the archaeology, which was readily picked up by both the multi-temporal airborne LiDAR derived CHMs and the aerial photography.

It is evident that at this "difficult" Diddington Clay field, the lack of contrast in canopy height relative to differences seen in LAI of the canopy manifested itself in both the multi-temporal airborne LiDAR derived CHMs (Figure 5). For both the 2011 and 2012 surveys, the models were able to detect only some areas of archaeology, some of which was different between the years; archaeology was more apparent in the 2011 oilseed rape crop. Note also that both these years had extreme weather (2011, very wet and 2012, very dry); unfortunately, the influence of this on the results is inconclusive since the planted crop differed between the years. At both dates, the multi-temporal airborne LiDAR derived CHM performed better than the aerial photographs, with the latter displaying very little contrast at all, although some of this may be spurious due to the close alignment of the cultivation patterns in the field and the archaeological features.

The multi-temporal airborne LiDAR derived CHM for Quarry Field, Harnhill (Figure 6), was seen to be extremely good at identifying archaeological features despite the soil being deemed "difficult" clay. This is supported by the field measurements where there was a clear increase in vegetation height over the archaeology. The pronounced contrast at this site between the vegetation canopy over the archaeology and the background is also present in the aerial photographs. However, the post medieval field boundary present at Cherry Copse (Figure 7) was not so easily discernable in the CHM, although linear features created by enclosures and trackways from rearing outdoor pigs in 2008 are clearly visible. This is also the case in the aerial photographs. This field has no supporting transect survey since the crop was impenetrable.

Since the results shown in Figures 4–7 are so incumbent on the DTM produced from the airborne LiDAR datasets captured in March 2012 (*i.e.*, when the earth was "bare") and this had been passed through a uniform low-pass filter, the filtered DTM was subtracted from the unfiltered DTM to illustrate the impact of this filtering, as the difference between the surface represents what had been added or removed by filtering (Figure 8). The left part of the image shows an immature oilseed rape crop with a crown height of c. 0.2 m. In the image, the area to the right has been recently ploughed, harrowed, and drilled for a maize crop which has not yet germinated.

Table 2. Condition of the state of the crop at each field study site during data acquisition.

Site	Date	Crop	Condition
Diddington T1	14 June 2011	Winter wheat	Flowering
Diddington T1	23 March 2012	Oilseed rape	Before stem elongation
Diddington T1	20 June 2012	Oilseed rape	Fruiting
Diddington Clay Field	14 June 2011	Oilseed rape	Fruiting
Diddington Clay Field	23 March 2012	Winter wheat	Tillers formed
Diddington Clay Field	20 June 2012	Winter wheat	Flowering
Harnhill Quarry Field	23 March 2012	Bare Soil	Drilled
Harnhill Quarry Field	20 June 2012	Spring wheat	Flowering
Harnhill Cherry Copse	23 March 2012	Pasture	Heavily grazed
Harnhill Cherry Copse	20 June 2012	Pasture	Mature meadow

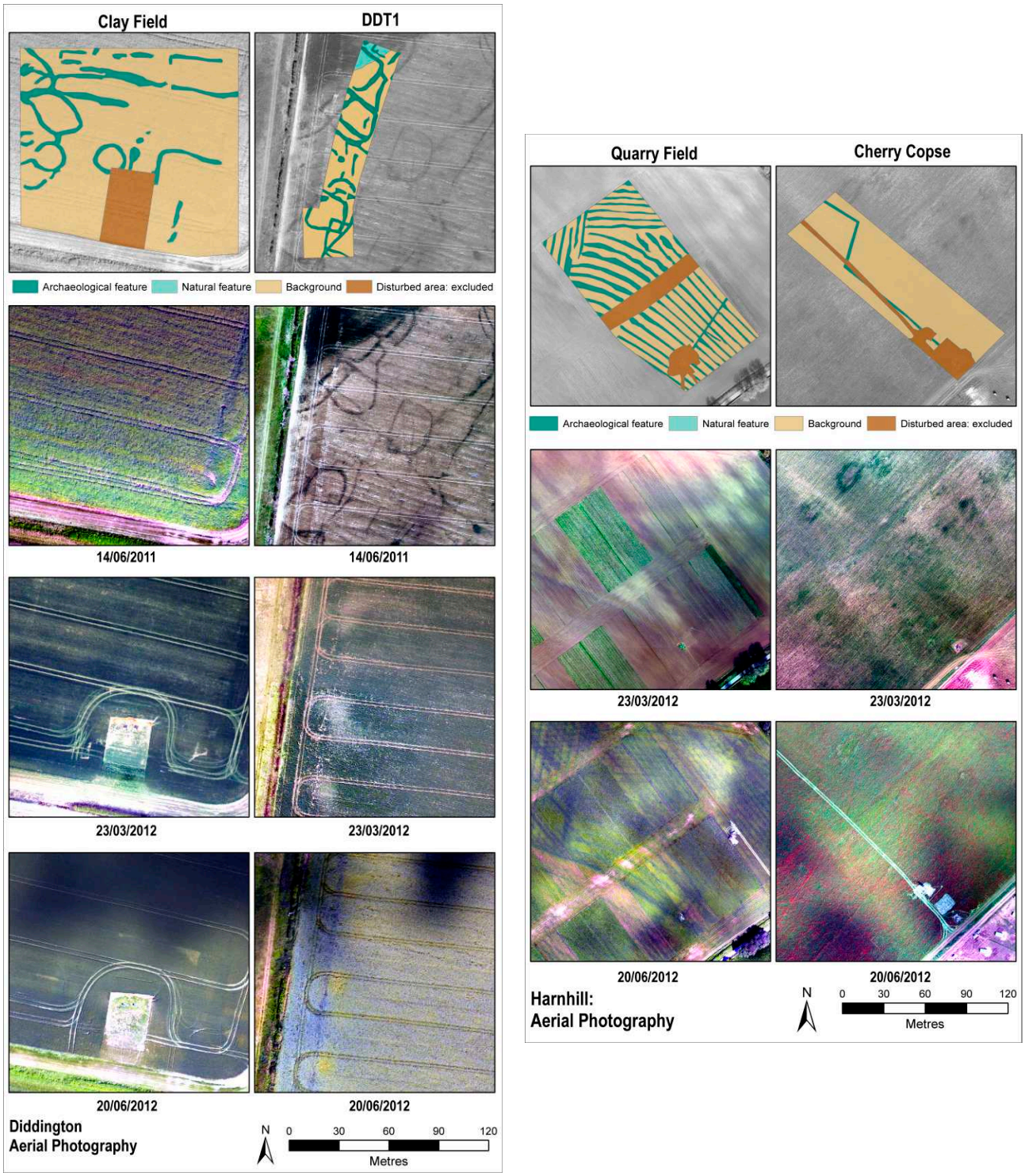

Figure 2. Magnetometer survey results for each of the four fields under investigation (top box in each column) and the corresponding aerial photography taken for each date that NERC ARSF surveyed each site. Note (i) that an ARSF survey was not undertaken in June 2011 for the Harnhill site and (ii) areas that have been disturbed at the Clay field at Diddington and both fields at Harnhill.

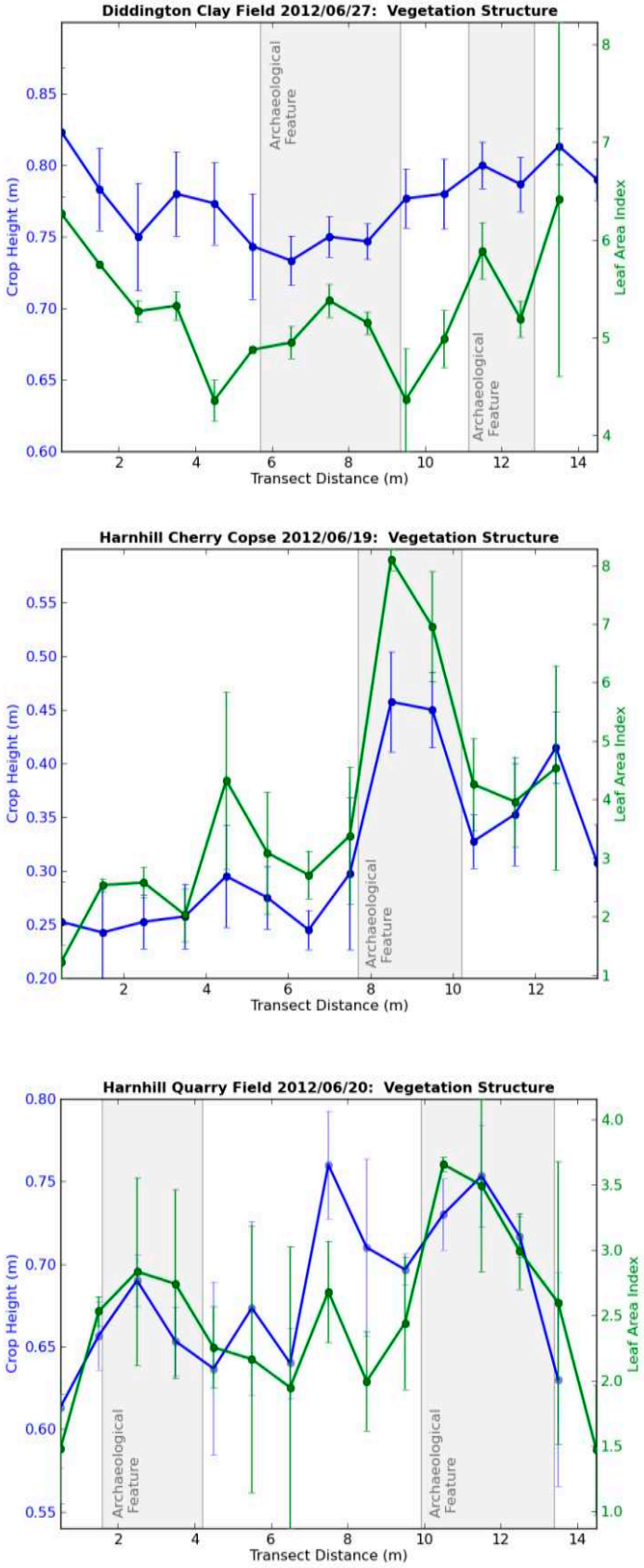

Figure 3. Profiles of vegetation height and LAI, June 2012 (mean and standard deviation). Note: no data available for DDT1 field as the crop was too dense and tall to access.

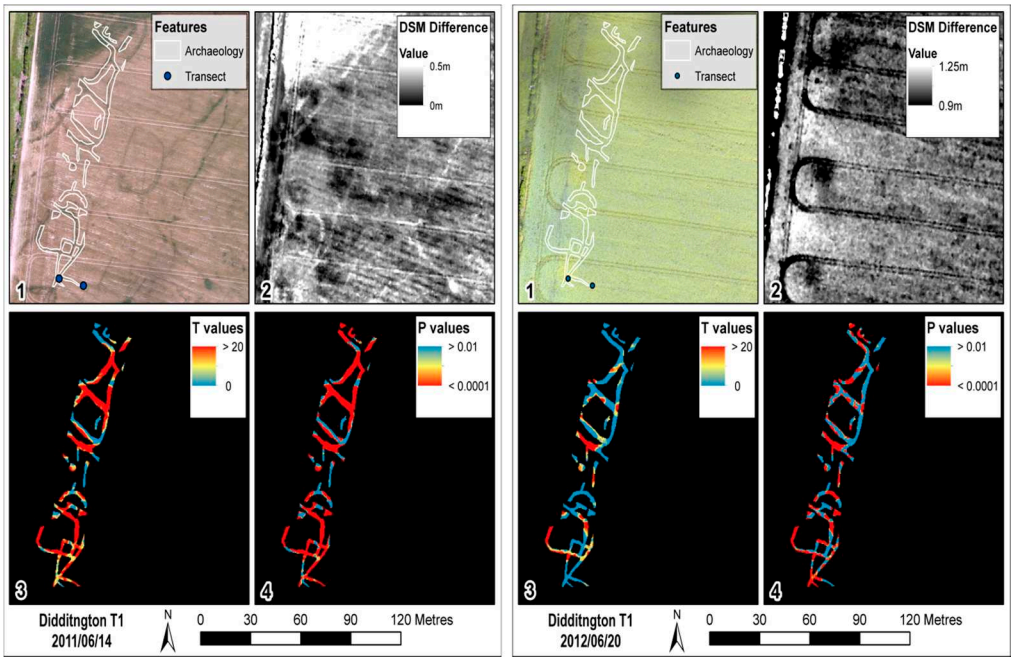

Figure 4. Multi-temporal airborne-LiDAR derived CHM for Diddington DDT1 field for Junes 2011 and 2012. (1) For comparison, aerial photography showing the locations of the archaeological features overlaid by those identified by magnetometer survey; (2) CHM data (referred to as difference in DSMs); (3) *T*-values indicating the strength of the localised contrast between the archaeological features and the background as exhibited by the CHM; (4) *P*-values indicating the localised statistical significance of the contrast.

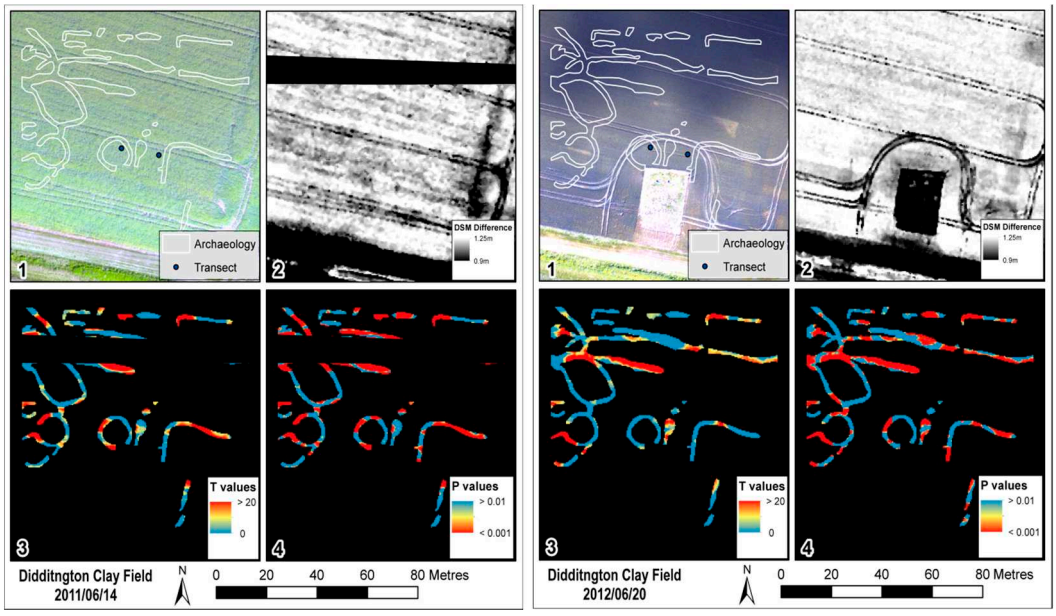

Figure 5. Multi-temporal airborne-LiDAR derived CHM for Diddington Clay field for Junes 2011 and 2012. (1) For comparison, aerial photography showing the locations of the archaeological features overlaid by those identified by magnetometer survey; (2) CHM data (referred to as difference in DSMs); (3) *T*-values indicating the strength of the localised contrast between the archaeological features and the background as exhibited by the CHM; (4) *P*-values indicating the localised statistical significance of the contrast.

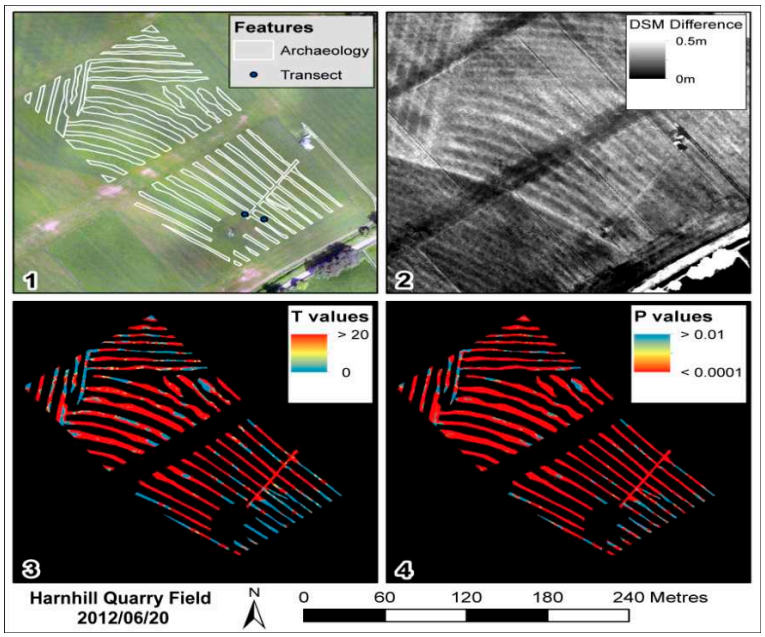

Figure 6. Multi-temporal airborne-LiDAR derived CHM for Harnhill Quarry Field for June 2012. (1) For comparison, aerial photography showing the locations of the archaeological features overlaid by those identified by magnetometer survey; (2) CHM data (referred to as difference in DSMs); (3) *T*-values indicating the strength of the localised contrast between the archaeological features and the background as exhibited by the CHM; (4) *P*-values indicating the localised statistical significance of the contrast.

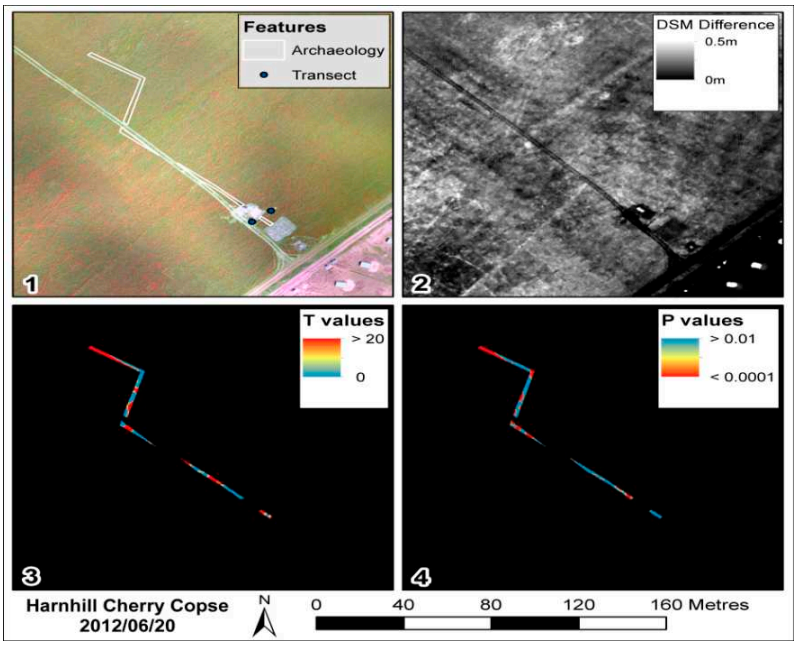

Figure 7. Multi-temporal airborne-LiDAR derived CHM for Harnhill Cherry Copse for June 2012. (1) For comparison, aerial photography showing the locations of the archaeological features overlaid by those identified by magnetometer survey; (2) CHM data (referred to as difference in DSMs); (3) *T*-values indicating the strength of the localised contrast between the archaeological features and the background as exhibited by the CHM; (4) *P*-values indicating the localised statistical significance of the contrast.

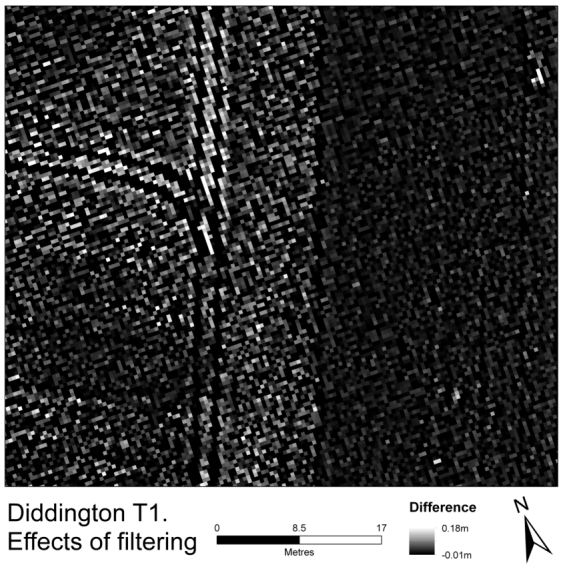

Figure 8. Result of examination of the impact of spatial filtering on the resultant DTM used to produce the multi-temporal airborne LiDAR derived CHMs at the Diddington site.

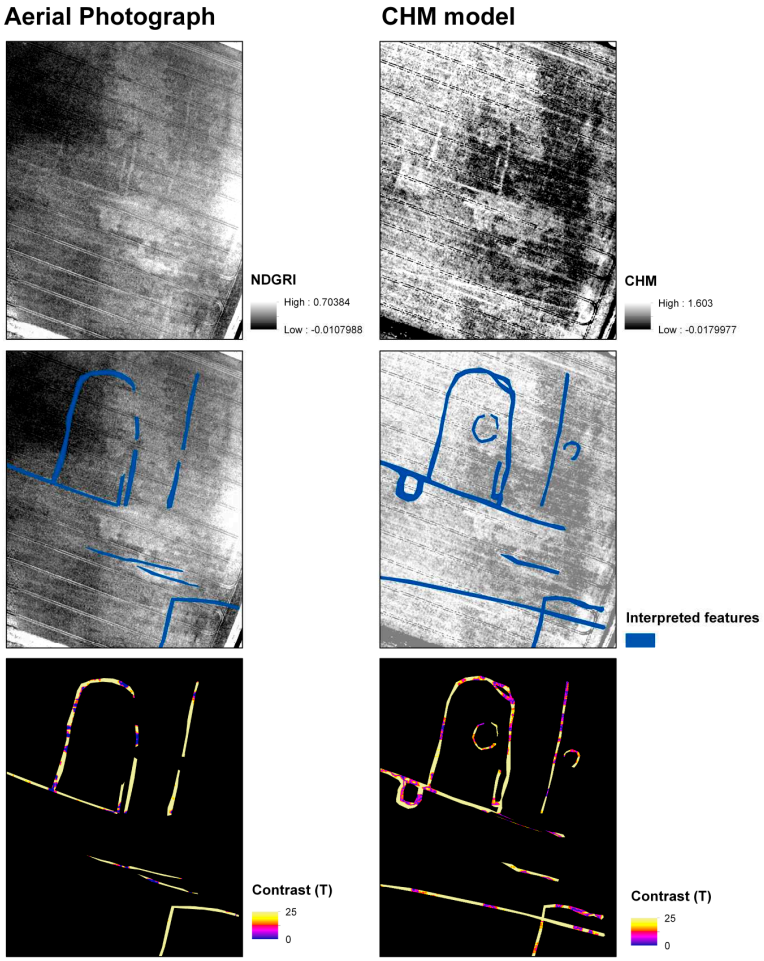

Figure 9. Comparison of the CHM method to NDGRI ortho-imagery for detecting previously unrecorded archaeological potential. This demonstrates that, while both methods can detect vegetation marks of archaeological potential, the CHM provides better definition of more features than the aerial photograph.

The test on the suitability of the multi-temporal airborne LiDAR derived CHM method for the detection of vegetation marks for archaeological prospection at the sites 200 m west of Harnhill Quarry Field revealed (Figure 9) a number of linear vegetation marks indicative of fragments of enclosures forming part of relict field systems. In general, the CHM subjectively performed slightly better, as it was possible to discern a greater overall length of linear features. In addition, it was possible to identify annular features possibly representative of prehistoric structures which were not visible in the aerial photography. Evaluations of contrasts using the method described above indicated that the overall strength of the contrast was similar in both methods. This, along with a qualitative examination of the CHM for each field, revealed a variation in performance across the sites and over time in the ability of the multi-temporal airborne LiDAR derived CHM to discriminate areas of archaeology from non-archaeology. This indicates that both environmental conditions and crop type have a role to play in the success of using this approach for archaeological detection and further experiments are needed to discern optimal application.

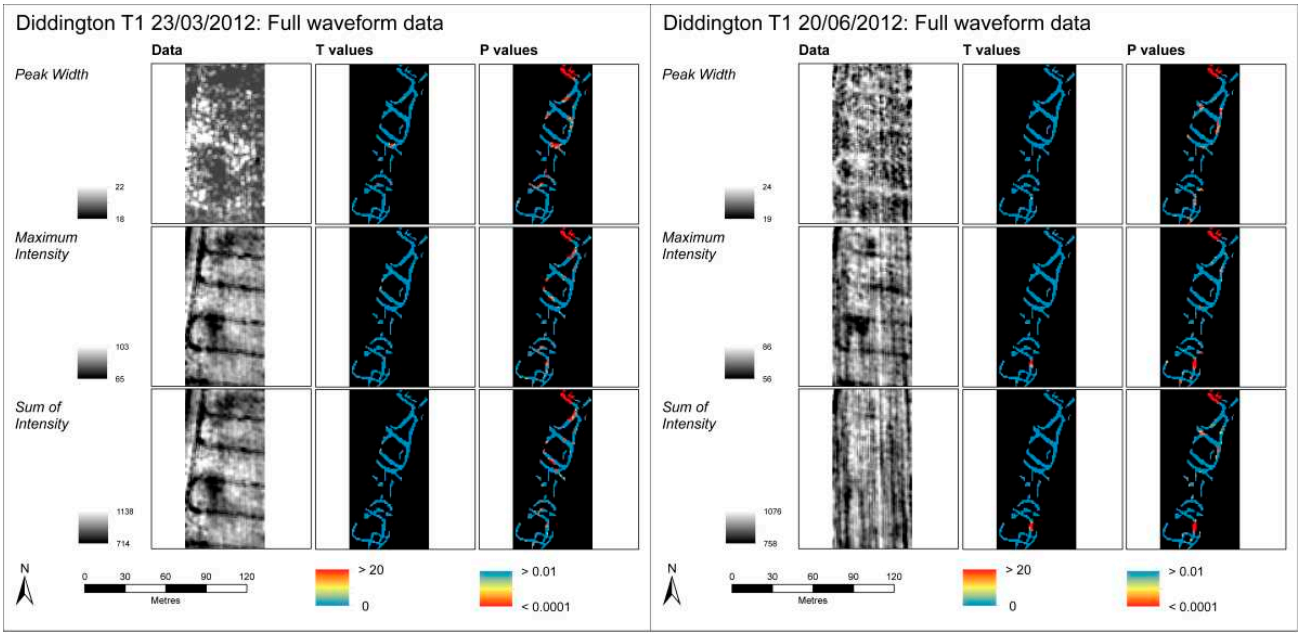

Figure 10. Metrics from airborne LiDAR full waveform data for Diddington T1 Field and corresponding *T*-values and *P*-values indicating localised contrast.

4.2. Archaeological Detection via Canopy Biomass Metrics Extracted From Full Waveform LiDAR

The results illustrating the potential for archaeological detection using canopy biomass metrics (peak width, maximum intensity, and sum of intensity of the extracted waveform) derived from full waveform airborne-LiDAR data are displayed in Figures 10–13. Clear contrast between the neighboring pixels is indicated when there is red in both the *T*-value and *P*-value images, and it is at these locations that archaeological residues are proxied.

In addition to these quantitative analyses, the qualitative examination of the resultant metric images reveal features present in the fields that are the result of agricultural practices (e.g., tram lines) for all fields across both acquisition dates (March and June 2012) and this is particularly apparent using the maximum intensity metric. Where there are discernable differences in the response as a result of the

presence of archaeology (though on the whole this is limited in comparison with that evident in the CHM and aerial photographs), this is most readily apparent using the peak width metric. This is supported by the quantitative analyses results, particularly at Harnhill Quarry field in the June 2012 acquisition.

Figure 14 displays the direct comparison of the aerial photographs, multi-temporal airborne LiDAR derived CHM, and the full waveform (FWF) derived peak width metric for the Quarry field at Harnhill, illustrating the limited ability of these data in comparison to the aerial photographs and the CHMs. As such, the use of full waveform LiDAR data is not recommended for use in this way.

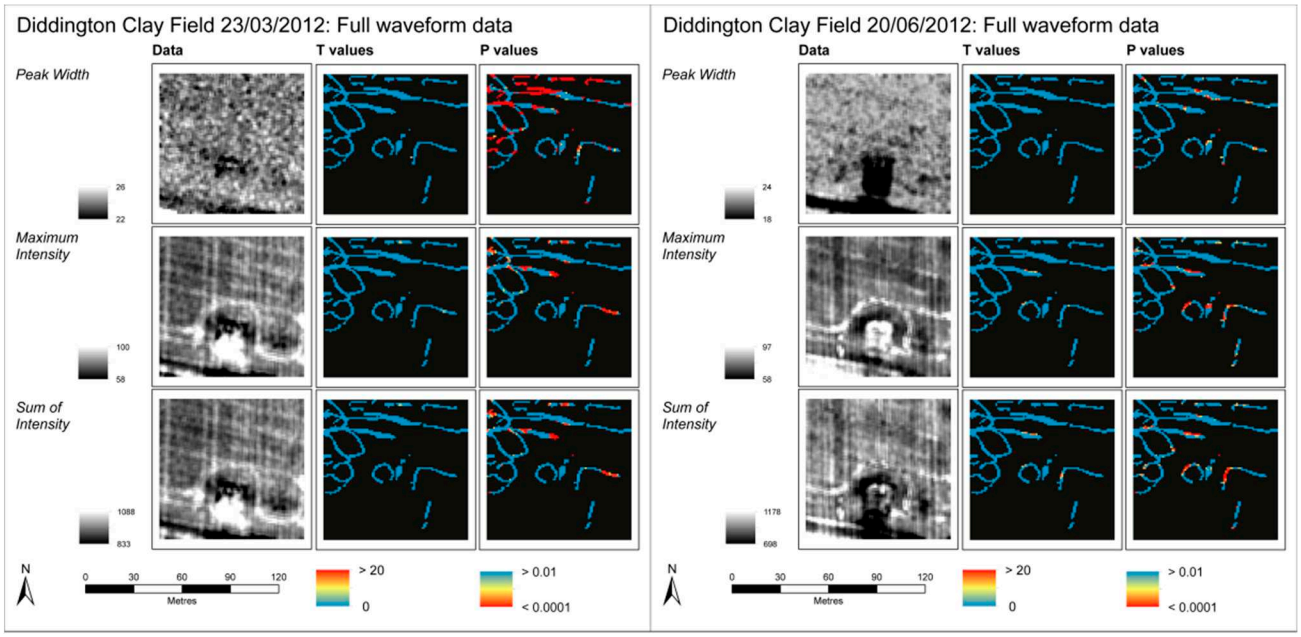

Figure 11. Metrics from airborne LiDAR full waveform data for Diddington Clay Field and *T*-values and *P*-values indicating localised contrast.

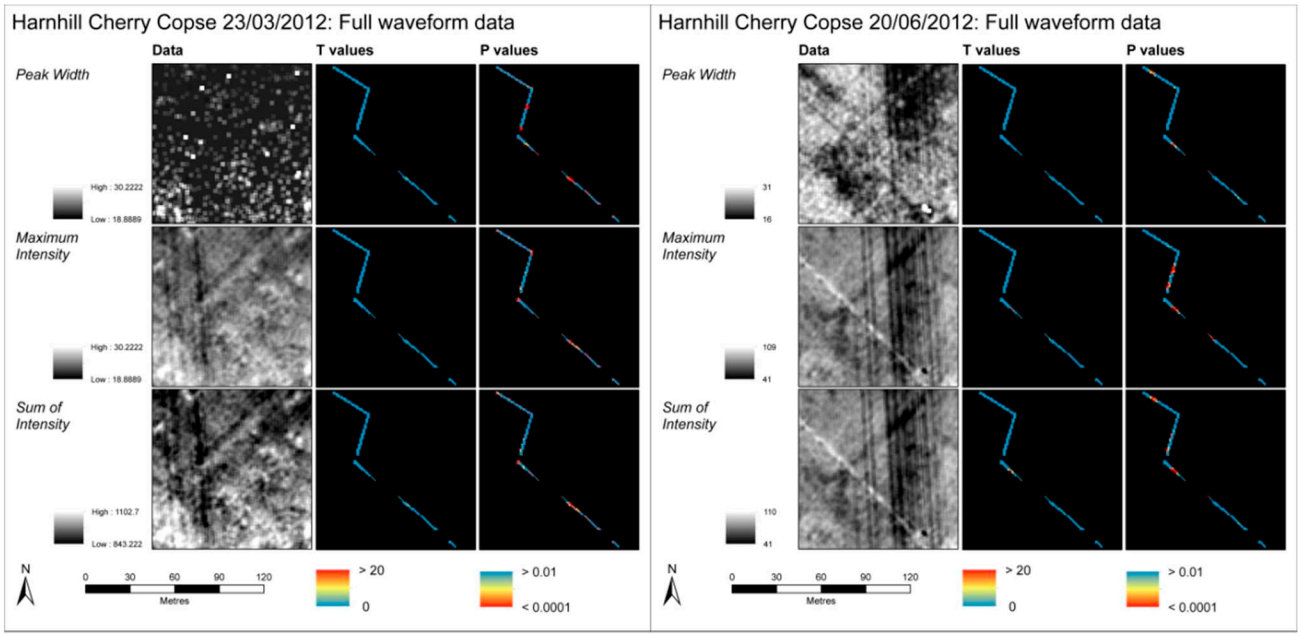

Figure 12. Metrics from airborne LiDAR full waveform data for Harnhill Cherry Copse field and *T*-values and *P*-values indicating localised contrast.

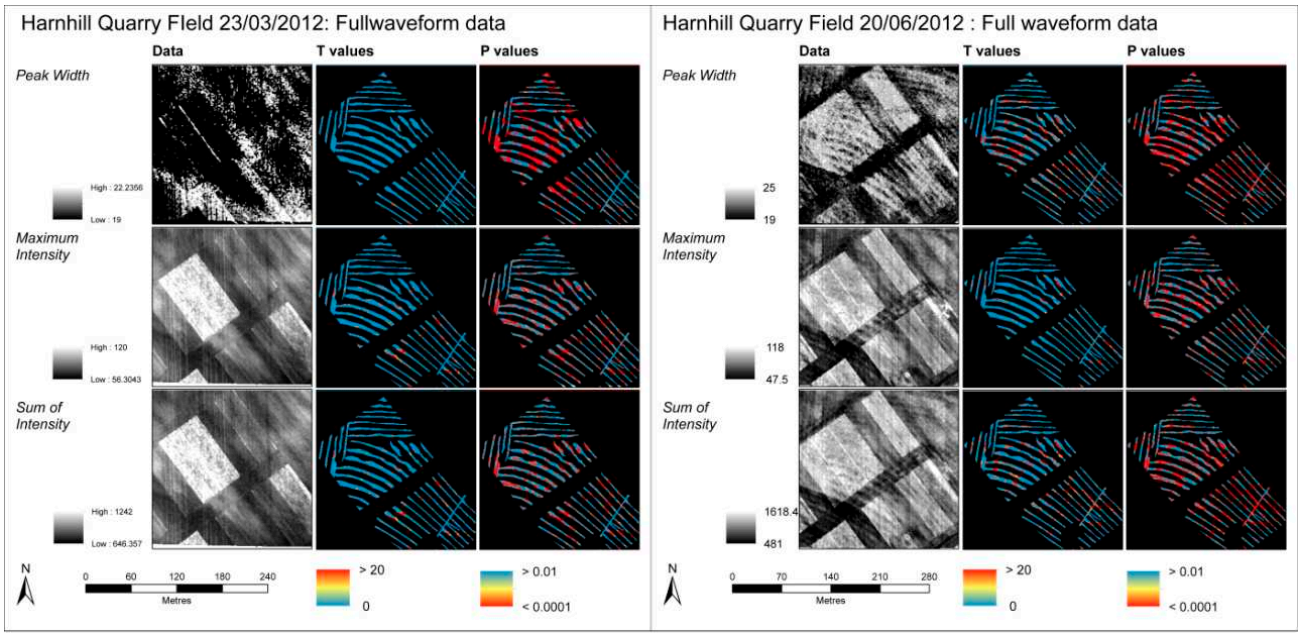

Figure 13. Metrics from airborne LiDAR full waveform data for Harnhill Quarry field and *T*-values and *P*-values indicating localised contrast.

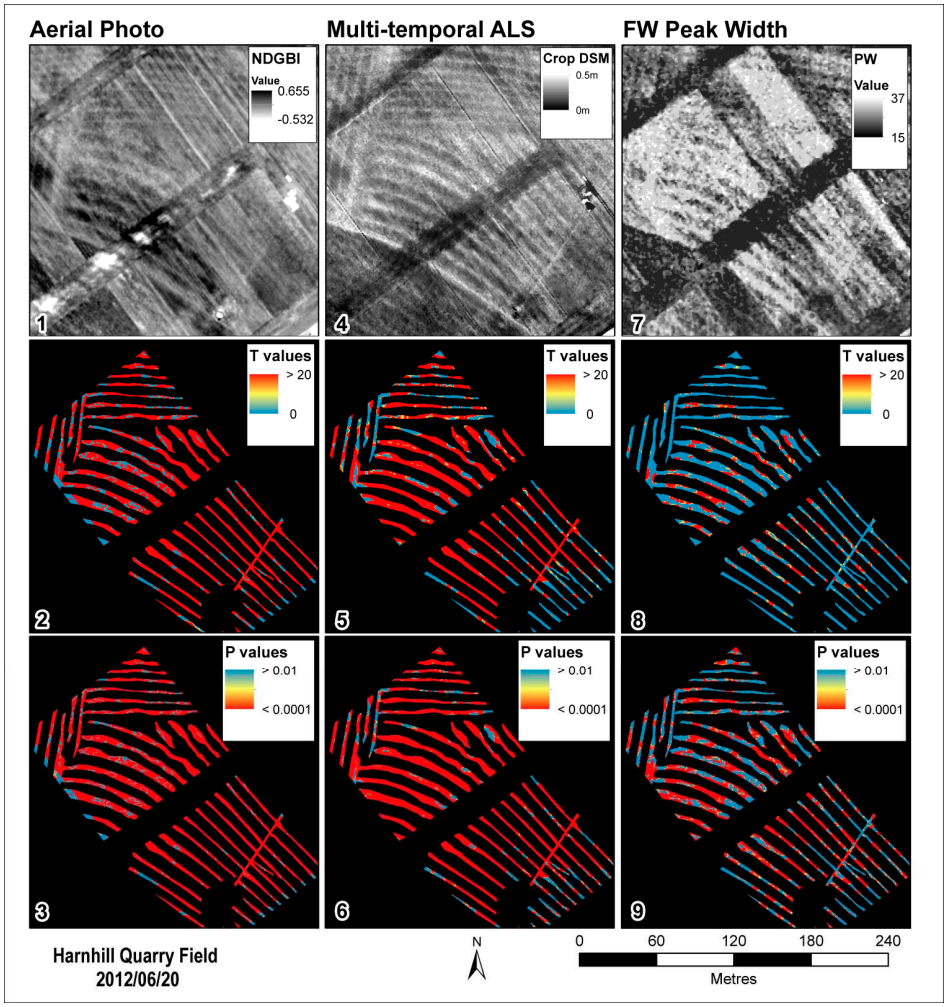

Figure 14. Harnhill Quarry field—Comparison between aerial photography, multi-temporal derived CHM and FWF metric data. *T*-values and *P*-values indicate localised contrast.

5. Discussion

This study explored the value of airborne LiDAR data for detecting archaeological features, using vegetation as a proxy for any differences in soil properties arising due to the presence of archaeological features. The conditions that give rise to optimal contrast in vegetation are a complex interaction of local conditions. This study attempts to unpick these in an experimental setting. Across different sites with different vegetation types, on different soils, with different climate and weather, it has been demonstrated that, where the presence of archaeology manifested itself in biomass variability in the overlying vegetation (as represented by LAI and/or height), this could be detected to varying extents in the airborne LiDAR data. Of the two approaches investigated, it was that which utilises multi-temporal airborne LiDAR discrete return data to produce canopy height models that is recommended for future consideration. Where there was a change in the canopy biophysical properties, this was also discernable in the CHMs and this was particularly evident the in oil seed rape crop in the Diddington DDT1 field, which has a soil comprising free-draining river deposits over Oxford Clay (Figure 4), as well as in the spring wheat crop in the Harnhill Quarry field which has limestone Cornbrash soil on a clayey signet member (Figure 6). The other two fields exhibited less contrast between CHM over archaeology *vs.* non-archaeology. In both the field transect data (Figure 3) and the CHM data (Figure 5) for the Diddington Clay Field, there was no real evidence of canopy changes due to the presence of archaeology, again illustrating the difficulty of detection in soils dominated by clay in this case, having a mid-Pleistocene till). The Harnhill Cherry Copse transect measurements show a sharp increase in crop height and LAI over the archaeology, but these were not picked up to the same extent in the CHM data due to some the crop being destroyed (trampled) in the intervening period between transect measurements and airborne survey (two days). Nevertheless, these field transect measurements indicate that the hypotheses put forward has validity, and it is a worthy endeavor to attempt to utilize airborne LiDAR in this way; this is the first study to attempt archeological prospection in this way, and these results demonstrate much potential, particularly once a base-line bare earth model is available for a site of interest.

This recommended use of multi-temporal airborne LiDAR data is not contingent on using the full waveform over discrete return data. Although the FWF data is capable of identifying the vegetation marks, the sensor is not capable of resolving the subtle contrast in the canopy as well as other methods; where contrasts are detectable using the FWF data, these were stronger and more apparent using the multi-temporal LiDAR derived CHM. This finding may change, however, with increasing data density [42]. However, the full waveform approach is attractive in that it requires only one survey date to be performed and does not require a base-line bare earth model. With both methods investigated here, a number of issues have been highlighted that require further investigation were this to develop into a more operational method to overcome the prospection bias that has arisen. These are discussed below.

5.1. Canopy Interactions

Given the footprint of the LiDAR sensor, it is suggested that the LAI is more important than the vegetation height in giving rise to any contrast seen in the modelled data. This was particularly apparent in the field measurements taken at the Diddington Clay Field in 2012, which illustrated that it was the LAI rather than the canopy height that differed between the archaeology and the background (Figure 3).

An increase in LAI represents an increase in vegetation coverage and a canopy that is more "closed". Theoretically, this provides a greater likelihood that the LiDAR pulse will interact with the canopy and that this will be reflected in the strength of the returned echo [43]. As to whether this is "detectable" in the LiDAR sensor (FWF or discrete) is dependent on how the returned signal is post-processed by the sensor system. We have assumed that the increase in LAI in turn increases the signal to noise ratio, which improves detection. The crop height, however, is measuring the extremity of individual plants within the canopy, whereas the field ceptometer measuring LAI and LiDAR-derived CHM are sampling multiple plants. Even with the generalizing effect of the 0.2 m footprint of the ALS pulses, typical planting densities in wheat for this study of 100 plants/m^2 mean that the probability of a return being digitized from the tallest point of the plant is comparatively low. In terms of the FWF LiDAR data, we would expect the peak width metric to be most sensitive to variations in the density and structure of the canopy. Increased LAI and crop height should mean that the recorded waveform is wider, as the pulse from the sensor takes longer to reach the ground. However, this is at the limit of the resolution of the FWF sensor. In addition, in very dense crops the pulse may not reach the ground at all, as was evident at Diddington DDT1 during summer 2012, which had the greatest peak width over the tramlines where the vegetation is least dense. FWF data allows the end user to have more control in the interpretation of the process [30]. Advances in processing methods, for instance [32,44], mean that extraction of metrics and computation of the data models improve in accuracy, giving the potential of improved archaeological detection due to more subtle contrast in canopy properties being resolved. Of course, using the full waveform, which offers increased pulse detection reliability, accuracy, and resolution [28–30], will, in turn, improve the accuracy of surface models produced and thus could be used in the multi-temporal fashion advocated here.

5.2. Multi-Temporal Airborne-LiDAR Datasets

DART has been fortunate enough to have access to a rich multi-temporal remote sensing dataset. Airborne LiDAR is a relatively expensive resource and justification is required to undertake even individual surveys. However, archives are being opened up that could be exploited. Moreover, laser scanners on UAV platforms have the potential to both increase the spatial resolution of the resultant model and reduce the cost of surveys. The increase in spatial resolution may be critical and will bridge the scale gap between the results observed in the sensor and the measurements recorded on the transect surveys. Irrespective of the cost implications, LiDAR surveys are less reliant on weather conditions than optical sensors. This is important in countries like the UK where the weather is a real issue for scientific aerial surveys [45]. The concept of mutli-temporal LiDAR studies is now taking hold due to more data now being available of the same study area [46,47]; however, this does mean that metadata concerning scanning hardware and post-processing is imperative to ensure consistency [48].

By statistically analysing the differences between a "bare earth" and "vegetation surface" model, it has been demonstrated that archaeological features can be detected. One benefit of the proposed technique is that once the "bare-earth" reference has been collected, these techniques can then be used with any subsequent data set assuming that there is no major change to the Earth's surface in the intervening time frame. By focusing on LAI and canopy structure variations, the proposed techniques have the potential to extend the utility of LiDAR surveys, as features can be detected that are neither

expressed as micro-topography or as intensity differences. This would mean that the underlying phenomena could only be captured by sensors that capture the contrast that are expressed in this way. The development of multi-spectral LiDAR [49] and the fusion of LiDAR data with spectral information from passive optical sensors [50] further extend the capabilities of these techniques. The integration of LiDAR and imaging spectroscopy techniques will help address the biases introduced by an over-reliance on the visual component of the electromagnetic spectrum [9,51–52]. An improvement in the science base, coupled with policy frameworks that facilitate changes in techniques with accompanying funding flexibility, are required to make the most of this. Other remote sensing devices and modes of operation have the potential to improve detection of archaeological residues (e.g., point clouds from cameras on board UAVs [53]), as their ability to detect subtly expressed contrasts affords the opportunity to both extend the temporal window for detection and detect subtly expressed features that cannot be detected using conventional aerial photography.

5.3. Data Acquisition Issues

Timing of data acquisition is a factor that needs to be considered. Diddington DDT1 in 2011 represented optimal conditions for data acquisition, where the vegetation marks were exceptionally clear due to the combination of drought [38], crop type, and soil type. However, during the same period, Diddington Clay Field, less than 1 km to the west, shows little contrast, a result of a different crop and clay soils where better moisture retention means that the variations in water resource constraint caused by archaeology and affecting the development of the crop are less pronounced [1]. On the other hand, 2012 was one of the wettest years on record, yet the clearest vegetation marks are evident in the clays at Harnhill Quarry field. Further work is required to resolve the problem of "what conditions" are appropriate for vegetation mark formation and, hence, detection with a particular sensor. Even with improvements in this knowledge, there is unlikely to be a single optimal window for data acquisition that can be applied across different soils and crops in the same geographic region. However, being able to extend the duration of the window within which these contrasts can be detected, as offered by airborne LiDAR, could provide significant operational flexibility.

5.4. Does Vegetation Mark Detection via Airborne LiDAR Add Value?

Conventional visible spectrum recording of archaeological vegetation marks rely on contrasts in colour and tone to identify potential archaeological features. Vegetation colour is the conflation of a number of properties: crop state, LAI, and absorption of visible light by photosynthetic and assistive pigments. Vegetation colour can vary markedly over short temporal windows as the crop adapts to changing resource availability or changes state. Canopy biomass (via height) is indicative of the ability of the soil to support a greater quantity of vegetation. Hence, vegetation colour differentials can be indicative of short term responses to localised conditions or vegetation states, whereas vegetation height differentials are more likely to indicate long-term developmental constraints reflecting differences in the soil. Where the soil and vegetation type is appropriate a canopy height approach has the potential to dramatically extend the window of opportunity for the detection of archaeological features. Furthermore, this may mean that this technique can be used to detect a range of different archaeological features on

different soils under different crops. This is a problem which has limited the use of large scale vertical surveys where the conditions for detection have more constraints.

This is exemplified by the surveys at Harnhill Quarry Field, which is located on clayey soils not generally conducive to vegetation mark formation. While both the aerial photography and the FWF data can identify the features in this field, the CHM method provides the greatest contrast. This indicates that this method has great potential for prospection of difficult soil, as if it can be used successfully in these difficult conditions, it is likely applicable elsewhere. This may be enhanced by the development of multi-spectral LiDAR systems [26]; if the instrument arrays can employ multiple wavelengths that facilitate the spectral separation of archaeological features, improved detection follows. Moreover, the increasingly common full waveforms approaches affords a unique perspective for feature detection, and could prove promising in fusion with other remotely sensed data, especially in heavily vegetated (wooded) environments. Deploying these sensors successfully requires a fine-grained understanding of the interactions between the underlying archaeology (its form and likely composition), environmental processes, and the vegetation canopy. To maximise impact, we need to understand not only the conditions under which sensors successfully detect archaeological features but also the overlap in detection between different sensors. If multiple sensors detect the same phenomena, then the most applicable sensor is the one that detects the phenomena over the greatest temporal window. Conversely, knowing that certain phenomena are only detected by a specific sensor will improve the justification for the deployment of that particular sensor. With this form of understanding there is the potential to both detect more subtly expressed features not detected using the more established aerial photography and, by virtue of the fairly limitless data acquisition conditions afforded by this active remote sensing method, to fully exploit temporal window for the detection of vegetation marks.

6. Conclusions

We have investigated methods for detecting archaeological features using multi-temporal airborne LiDAR and single-date full waveform LiDAR over vegetation. The majority of the contrasts between the archaeology and the background are a result of the differences in canopy biomass and in comparison with aerial photography. It was the multi-temporal airborne LiDAR used to produce a CHM that was best able to distinguish these contrasts. The LiDAR data does not provide information on the state of the crop beyond the biomass, however, and this may prove invaluable when used in conjunction with imaging spectroscopy. Using these sensors together provides the potential to improve our ability to detect archaeological features over using them individually. Once there is a "bare-earth" reference, these techniques can then be used with any subsequent data set assuming that there is no major change to the Earth's surface in the intervening time frame.

These novel approaches add significantly to the airborne LiDAR prospection repertoire, in that it allows the detection of archaeological features that are expressed neither in surface relief nor as spectral differences in the LiDAR intensity measurements. However, the timing of the data capture is important to maximise return invested in deploying airborne LiDAR and this will be dependent on soil type, vegetation type, and the preceding weather patterns. The proposed technique provides a mechanism to increase certainty of detection when employed in the increasingly multi-sensor approaches to heritage prospection and management, which combine aerial remote sensing and field verification on the ground.

Acknowledgements

The DART project (www.comp.leeds.ac.uk/dart) is supported by a Science and Heritage large research grant (award AH/H032673/1) from the Arts and Humanities Research Council (www.ahrc.ac.uk) and the Engineering and Physical Sciences Research Council (www.epsrc.ac.uk). NERC ARSF captured LiDAR and aerial photography and Geomatics Group Ltd also collected aerial photography. Many thanks go to Royal Agricultural University and Thornhill Estates for access permissions.

Author Contributions

This research was carried out as part of David Stott's PhD research supervised by the three co-authors. Of these Doreen Boyd and Anthony Beck wrote the article aided by Anthony Cohn in an editorial capacity. All authors commented on the manuscript and accepted the content.

Conflicts of Interest

The authors declare no conflict of interest.

References

1. Evans, R. The weather and other factors controlling the appearance of crop marks on clay and "difficult"soils. In *Populating Clay Landscapes*; Mills, J., Palmer, R., Eds.; Tempus: Stroud, UK, 2007; pp. 16–27.
2. Hejcman, M.; Smirz, Z. Cropmarks in stands of cereals, legumes and winter rape indicate sub-soil archeological features in the agricultural landscape of central Europe. *Agric. Ecosyst. Environ.* **2010**, *138*, 348–354.
3. Bennett, R.; Welham, K.; Hill, R.A.; Ford, A. Airborne spectral imagery for archaeological prospection in grassland environments—An evaluation of performance. *Antiquity* **2013**, *87*, 220–237.
4. Beck, A.R. Archaeological applications of multi/hyper-spectral data—Challenges and potential. In *Remote Sensing for Archaeological Heritage Management*; Cowley, D.C., Ed.; Europae Archaeologia Consilium: Budapest, Hungary, 2011; pp. 87–98.
5. Jones, R.J.A.; Evans, R. *Soil and Crop Marks in the Recognition of Archaeological Sites by Air Photography*; Aerial Reconnaissance for Archaeology: London, UK, 1975.
6. Brophy, K.; Cowley, D. *From the Air: Understanding Aerial Archaeology*; Tempus: Stroud, UK, 2005.
7. Hejcman, M.J.; Ondracek, J.; Smrz, Z. Ancient waste pits with wood ash irreversibly increase crop production in central Europe. *Plant Soil* **2011**, *339*, 341–350.
8. Bennett, R.; Welham, K.; Hill, R.A.; Ford, A. The application of vegetation indices for th prospection of archaeological features in grass-dominated environments. *Archaeol. Prospect.* **2012**, *19*, 209–218.

9. Verhoeven, G.; Doneus, M.; Atzberger, C.; Wess, M.; Rus, M.; Pregesbauer, M.; Briese, C. New approaches for archaeological feature extraction of airborne imaging spectroscopy data. In Proceedings of the 10th International Conference on Archaeological Prospection, Vienna, Austria, 29 May–2 June 2013; pp. 13–15.
10. Bennett, R.; Welham, K.; Hill, R.A.; Ford, A. A comparison of visualisation techniques for models created airborne laser scanned data. *Archaeol. Prospect.* **2012**, *19*, 41–48.
11. Cowley, D.C. A case study in the analysis of patterns of aerial reconnaissance in a lowland area of southest Scotland. *Archaeol. Prospect.* **2002**, *9*, 255–265.
12. Mills, J. Bias and the world of the vertical aerial photograph. In *From the Air: Understanding Aerial Archaeology*; Brophy, K., Cowley, D., Eds.; Tempus: Stroud, UK, 2005; pp. 117–126.
13. Cowley, D.C.; Dickson, A.L. Clays and "difficult Soils" in Eastern and Southern Scotland: Dealing with the gaps. In *Populating Clay Landscapes*; Mills, J., Palmer, R., Eds.; Tempus: Gloucester, UK, 2007; pp. 43–54.
14. Rowlands, A.; Sarris, A. Detection of exposed and subsurface archaeological remains using multi-sensor remote sensing. *J. Archaeol. Sci.* **2007**, *34*, 795–803.
15. Verhoeven, G.J. Near-infrared aerial crop mark archaeology: From its historical use to current digital implementations. *J. Archaeol. Method Theory* **2011**, *19*, 132–160.
16. Bernardini, F.; Sgambati, A.A.; Montagnari, M.; Kokelj, M.; Zaccaria, C.; Micheli, R.; Fragiacomo, A.; Tiussi, C.; Dreossi, D.; Tuniz, C.; *et al.* Airborne LiDAR application to karstic areas: The example of Trieste province (north-eastern Italy) from prehistoric sites to Roman forts. *J. Archaeol. Sci.* **2013**, *40*, 2152–2160.
17. Masini, N.; Lasaponara, R. Airborne lidar in archaeology: Overview and a case study. In Proceedings of the 13th International Conference, Ho Chi Minh City, Vietnam, 24–27 June 2013.
18. Challis, K.; Kokalj, Z.; Kincey, M.; Moscrop, M.; Howard, A.J. Airborne lidar and historic environment records. *Antiquity* **2008**, *82*, 1055–1064.
19. Chase, A.F.; Chase, D.Z.; Weishampel, J.F.; Drake, J.B.; Shrestha, R.L. Slatton, C.; Awef, J.J.; Carter, W.E. Airborne LiDAR, archaeology, and the ancient Maya landscape at Caracol, Belize. *J. Archaeol. Sci.* **2011**, *38*, 387–398.
20. Evans, D.; Fletcher, R.J.; Pottier, C.; Chevanc, J.-B.; Souti, D.; Tand, B.S.; Imd, S.; Ead, D.; Tind, T.; Kimd, S.; *et al.* Uncovering archaeological landscapes at Angkor using lidar. *Proc. Natl. Acad. Sci. USA* **2013**, *110*, 12595–12600.
21. Johnson, K.M.; Ouimet, W.B. Rediscovering the lost archaeological landscape of southern New England using airborne light detection and ranging (LiDAR). *J. Archaeol. Sci.* **2014**, *43*, 9–20.
22. Cui, Y.; Zhao, K.; Fan, W.; Xu, X. Using lidar to retreive crop structural parameters. In Proceedings of the 2010 IEEE International Geoscience and Remote Sensing Sympsium IGARSS, Honolulu, HI, USA, 25–30 July 2010.
23. Challis, K.; Carey, C.; Kincey, M.; Howard, A.J. Airborne lidar intensity and geoarchaeological prospection in river valley floors. *Archaeol. Prospect.* **2011**, *18*, 1–13.
24. Challis, K.; Carey, C.; Kincey, M.; Howard, A.J. Assessing the preservation potential of temperate, lowland alluvial sediments using airborne lidar intensity. *J. Archaeol. Sci.* **2011**, *38*, 301–311.

25. Briese, C.; Doneus, M.; Verhoeven, G. Radiometric calibration of ALS data for archaeological interpretation. In Proceedings of the 10th International Conference, Vienna, Austria, 29 May–2 June 2013.
26. Briese, C.; Pfennigbauer, M.; Ullrich, A.; Doneus, M. Radiometric information from airborne Laser scanning for archaeological prospection. *Int. J. Herit. Digit. Era* **2014**, *3*, 159–178.
27. Höfle, B.; Hollaus, M.; Hagenauer, J. Urban vegetation detection using radiometrically calibrated small-footprint full-waveform airborne LiDAR data. *ISPRS J. Photogramm. Remote Sens.* **2012**, *67*, 134–147.
28. Doneus, M.; Briese, C. Full-waveform airborne laser scanning as a tool for archaeological reconnaissance. *BAR Int. Ser.* **2006**, *1568*, 99–105.
29. Doneus, M.; Briese, C.; Fera, M.; Janner, M. Archaeological prospection of forested areas using full-waveform airborne laser scanning. *J. Archaeol. Sci.* **2008**, *35*, 882–893.
30. Lasaponara, R.; Coluzzi, R.; Masini, N. Flights into the past: Full-waveform airborne laser scanning data for archaeological investigation. *J. Archaeol. Sci.* **2011**, *38*, 2061–2070.
31. Mallet, C.; Bretar, F. Full-waveform topographic lidar: State-of-the-art. *ISPRS J. Photogramm. Remote Sens.* **2009**, *64*, 1–16.
32. Wagner, W.; Ullrich, A.; Ducic, V.; Melzer, T.; Studnicka, N. Gaussian decomposition and calibration of a novel small-footprint full-waveform digitising airborne laser scanner. *ISPRS J. Photogramm. Remote Sens.* **2006**, *60*, 100–112.
33. Mallet, C.; Bretar, F.; Soergel, U. Analysis of full-waveform lidar data for classification of urban areas. *Photogramm. Fernerkund. Geoinf.* **2008**, *5*, 337–349.
34. Anderson, J.; Martin, M.; Dubayah, M.L.; Dubayah, R.; Hofton, M.; Hyde, P.; Peterson, B.; Blair, J.; Knox, R. The use of waveform LiDAR to measure northern temperate mixed conifer and deciduous forest structure in New Hampshire. *Remote Sens. Environ.* **2006**, *105*, 248–261.
35. Heinzel, J.; Koch, B. Exploring full-waveform LiDAR parameters for tree species classification. *Int. J. Appl. Earth Obs. Geoinf.* **2011**, *13*, 152–160.
36. Buddenbaum, H.; Seeling, S.; Hill, J. Fusion of full-waveform lidar and imaging spectroscopy remote sensing data for the characterization of forest stands. *Int. J. Remote Sens.* **2013**, *34*, 4511–4524.
37. DART Project. Available online: www.comp.leeds.ac.uk/dart (accessed on 16 July 2014).
38. UK Meteorological Office. Available online: http://www.metoffice.gov.uk/climate/uk/summaries (accessed on 16 July 2014).
39. DART Datasets. Available online: http://dartportal.leeds.ac.uk/dataset (accessed on 16 July 2014).
40. Zhang, G.; Ganguly, S.; Nemani, R.R.; White, M.A.; Miles, C.; Hashimoto, H.; Wang, W.; Saatchi, S.; Yuf, Y.; Myneni, R.G. Estimation of forest aboveground biomass in California using canopy height and leaf area index estimated from satellite data. *Remote Sens. Environ.* **2014**, *151*, 44–56.
41. Bespoke Python Software. Available online: https://github.com/dav-stott/2014_Lidar_Paper/tree/master (accessed on 16 July 2014).
42. Lin, Y.-C.; Mills, J.P. Factors influencing pulse width of small footprint, full waveform airborne laser scanning data. *Photogramm. Eng. Remote Sens.* **2010**, *76*, 49–59.

43. Morsdorf, F.; Kotz, B.; Meier, E.; Itten, K.I.; Allgower, B. Estimation of LAI and fractional cover from small footprint airborne laser scanning data based on gap fraction. *Remote Sens. Environ.* **2006**, *104*, 50–61.
44. Zhuang, W.; Mountrakis, G. An accurate and computationally efficient algorithm for ground peak identification in large footprint waveform LiDAR data. *ISPRS J. Photogramm. Remote Sens.* **2014**, *95*, 81–92.
45. Armitage, R.P.; Alberto Ramirez, F.; Mark Danson, F.; Ogunbadewa, E.Y. Probability of cloud-free observation conditions across Great Britain estimated using MODIS cloud mask. *Remote Sens. Lett.* **2013**, *4*, 427–435.
46. Blackburn, G.A.; Latif, Z.; Boyd, D.S. Forest disturbance and regeneration: A mosaic of discrete gap dynamics and open matrix regimes? *J. Veg. Sci.* **2014**, *25*, 1341–1354.
47. Englhart, S.; Jubanski, J.; Siegert, F. Quantifying dynamics in tropical peat swamp forest biomass with multi-temporal LiDAR datasets. *Remote Sens.* **2013**, *5*, 2368–2388.
48. Hopkinson, C.; Chasmer, L.E.; Hall, R.J. The uncertainty in conifer plantation growth prediction from multitemporal lidar datasets. *Remote Sens. Environ.* **2008**, *112*, 1168–1180.
49. Pfennigbauer, M.; Ullrich, A. Multi-wavelength airborne laser scanning. In Proceedings of the 2011 International Lidar Mapping Forum, ILMF, New Orleans, LA, USA, 7–9 February 2011.
50. Mesas-Carrascosa, F.J.; Castillejo-González, I.L.; de la Orden, M.S.; Porras, A.G.-F. Combining LiDAR intensity with aerial camera data to discriminate agricultural land uses. *Comput. Electron. Agric.* **2012**, *84*, 36–46.
51. Beck, A.R. Archaeological site detection: The importance of contrast. In Proceedings of the 2007 Annual Conference of the Remote Sensing and Photogrammetry Society, Newcastle, Australia, 11–14 September 2007; pp. 307–312.
52. Beck, A.; Wilkinson, K.; Philip, G. Some techniques for improving the detection of archaeological features from satellite imagery. *Proc. SPIE* **2007**, doi:10.1117/12.736704.
53. Rosnell, T.; Honkavaara, E. Point cloud generation from aerial image data acquired by a quadrocopter type micro Unmanned Aerial Vehicle and a digital still camera. *Sensors* **2012**, *12*, 453–480.